# The effectiveness and safety of X-PDT for cutaneous squamous cell carcinoma and melanoma

Lei Shi[‡,1] [iD], Pei Liu[‡,1], Jing Wu[2], Lun Ma[3], Han Zheng[3], Michael P Antosh[4,5], Haiyan Zhang[1], Bo Wang[1], Wei Chen**[,3] & Xiuli Wang*[,1]

[1]Institute of Photomedicine, Shanghai Skin Disease Hospital, Tongji University School of Medicine, Shanghai, 200443, PR China
[2]Department of Computer Science & Statistics, University of Rhode Island, 9 Greenhouse Rd, Kingston, RI 02881, USA
[3]Department of Physics, the University of Texas at Arlington, Arlington, TX 76019-0059, USA
[4]Physics Department, University of Rhode Island, 2 Lippitt Rd, Kingston, RI 02881, USA
[5]Institute for Brain & Neural Systems, Brown University, 184 Hope St, Providence, RI 02912, USA
*Author for correspondence: wangxiuli_1400023@tongji.edu.cn
**Author for correspondence: weichen@uta.edu
‡ Authors contributed equally

**Aim:** To clarify the effectiveness and safety of x-ray-activated photodynamic therapy (X-PDT) for cutaneous squamous cell carcinoma (SCC) and melanoma. **Materials & methods:** Copper-cysteamine nanoparticles were used as a photosensitizer of X-PDT. The dark toxicity and cytotoxicity were studied *in vitro.* Tumor volume, microvessel density and acute toxicity of mice were evaluated *in vivo.* **Results:** Without x-ray irradiation, copper-cysteamine nanoparticles were nontoxic for keratinocyte cells. XL50 cells (SCC) were more sensitive to X-PDT than B16F10 cells (melanoma). X-PDT successfully inhibited the growth of SCC *in vivo* ($p < 0.05$), while the B16F10 melanoma was resistant. Microvessel density in SCC tissue was remarkably reduced ($p < 0.05$). No obvious acute toxicity reaction was observed. **Conclusion:** X-PDT is a safe and effective treatment for SCC.

Photodynamic therapy (PDT) combines the actions of a photosensitizer, light and oxygen into a relatively novel noninvasive treatment modality for cutaneous tumors [1]. In the body, tumor cells and vascular endothelial cells preferentially absorb more photosensitizers than other cells. When exposed to light, photosensitizers absorb the photonic energy and transfer it to nearby triplet oxygen, resulting in the generation of reactive oxygen species (ROS). ROS can damage or kill tumor cells and vascular endothelial cells directly, by the necrosis and apoptosis pathways [2]. As a result of the damage caused by ROS, the antitumor immune response is elicited to further eliminate tumor cells, blocking tumor vessels and leading to the deprivation of nutrients for the tumor. In recent years, studies on the immune response in PDT attracted more attention than vascular effect in the treatment of cancers [2,3]; however, it cannot be denied that vascular effect is a very important advantage of PDT for cancers [4,5]. In particular, the vascular effect can induce a quick inhibiting effect on solid tumors [6].

Based on its advantages of allowing repetitive applications to multiple lesions, nontrauma and excellent cosmetic results, PDT became a popular treatment for skin cancers, especially when surgery is unavailable [1]. PDT showed a remarkable effectiveness for the treatment of superficial cutaneous cancers, such as actinic keratosis, superficial basal cell carcinoma and Bowen's disease, also called cutaneous squamous carcinoma (SCC) *in situ* [1]. However, for invasive or massive SCC and melanoma, the effectiveness of conventional PDT is unsatisfactory. The possible main reasons are: poor tumor targeting of current photosensitizers [7]; low penetration depth of the activation light which is only 3 mm [8] – much shorter than the depth of common SCC or melanoma in the clinic; the tumor regrowth supported by the surviving deep tumor vessels [9] and the tumor resistances to the PDT [10,11].

Future Medicine
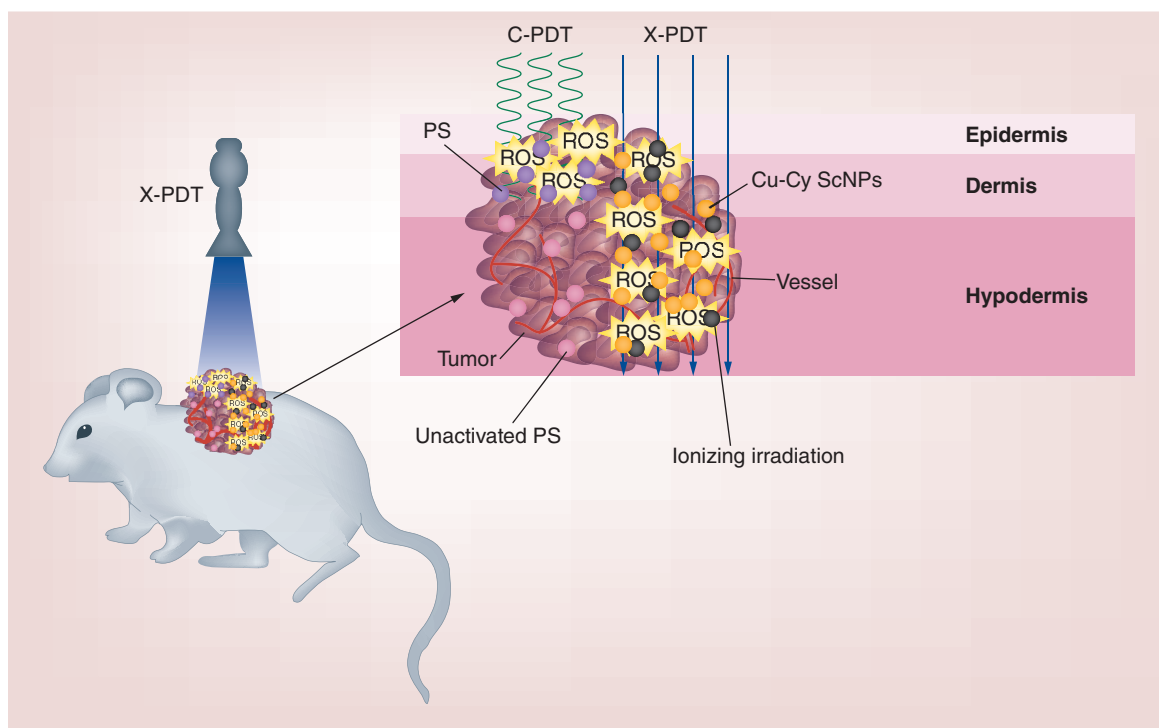
**Figure 1.    Schematic illustration of x-ray-activated photodynamic therapy with copper-cysteamine nanoparticles.** Compared with visible light, x-rays can penetrate through the epidermis and dermis to the hypodermis. Upon the irradiation of x-rays, ROS produced by Cu-Cy NPs and ionizing irradiation are generated in the whole tumor. The photodynamic effect and radiotherapy exert the antitumor effect at the same space and time to override tumor cell repairs and lead to the deep tumor vascular effect.
Cu-Cy NP: Copper-cysteamine nanoparticle; C-PDT: Conventional photodynamic therapy; PS: Photosensitizer; ROS: Reactive oxygen species; X-PDT: X-ray-activated photodynamic therapy.

Scintillator nanoparticle is a class of nanoparticles made of scintillator materials that are able to convert x-rays into visible fluorescence [12]. In recent years, more and more studies have utilized scintillator nanoparticles to load and deliver a photosensitizer for PDT [13–15]. In these nanoparticles, the scintillator substance and photosensitizers are close to each other. After the scintillator nanoparticles are exposed to x-rays, the energy of the x-rays is converted to photosensitizers by activating the fluorescence resonance energy transfer between scintillator substance and loaded photosensitizers [16]. Thus, x-rays are able to activate current photosensitizers indirectly [17,18]. Compared with visible light, x-rays have higher photon energies. They can penetrate through the epidermis and dermis to the hypodermis. The effective depth of x-rays is significantly deeper than visible light, as well as near-infrared light [19]. In addition to the tumor damage produced by PDT, the x-rays themselves could directly damage or kill tumor cells to enhance the effect of PDT (Figure 1). Nanoparticles are also able to enhance the tumor targeting of photosensitizers by the enhanced permeability retention effect [20,21].

However, the energy of the above X-PDT modality might be worn down in the complicated transfer procedures, resulting in photosensitizers that could not receive enough optical energy to generate adequate ROS for the tumor treatment. Copper-cysteamine nanoparticles (Cu-Cy NPs) were established by Chen and colleagues, and show an intense x-ray-excited luminescence [22,23]. More interesting is that Cu-Cy NPs can act as a photosensitizer to directly produce ROS upon the irradiation of x-rays. That means in this X-PDT model (Figure 1), Cu-Cy NPs did not need to transfer the energy absorbed from x-ray to another photosensitizer, implying an efficient energy conversion from light energy to chemical energy.

Cu-Cy NPs-mediated X-PDT was proven to be an effective modality for the treatment of breast cancer, colorectal cancer and hepatocellular carcinoma [22,24,25]. As in the clinic, skin cancers are the main indications of PDT, x-ray therapy or other phototherapies. Among them, the treatments on cutaneous SCC and melanoma are the most important challenges in the clinic. Therefore, in this study we evaluate the effectiveness and safety of Cu-Cy NPs-mediated X-PDT for treatment of cutaneous SCC and melanoma together.

## Materials & methods

### Preparation & characterization of Cu-Cy nanoparticles

Cu-Cy NPs were prepared at the University of Texas using the method as previously described in the literature [24]. Briefly, $CuCl_2 \cdot 2H_2O$ dissolved in deionized water was mixed with cysteamine and the PH value was adjusted to 8 using sodium hydroxide solution. After a 2-h period of stirring, the solution was heated to its boiling temperature for 30 min. The Cu-Cy NPs were obtained after centrifuging and washing the crude product with an ethanol solution five-times. Finally, the nanoparticles were dried in a vacuum oven overnight. A stock solution was made in phosphate-buffered saline at a concentration of 1 mg/ml. The solution was kept in the dark at -4°C. The morphology and particle size of Cu-Cy NPs were characterized using a transmission electron microscope (JEM-2100, Japan Electronics Co., Ltd., Tokyo, Japan).

### Cell culture

Human keratinocyte HaCaT cells and melanoma B16F10 cells were purchased from Shanghai Cell Bank (Shanghai, China). The primary cultured murine cutaneous SCC cell, XL50 cell line, was established from ultraviolet-induced SCC on SKH-1 hairless mice and stored at China Center for Type Culture Collection (CCTCC No: C201827, Wuhan, China) [26]. The above cells were cultured in Roswell Park Memorial Institute (RPMI) 1640 medium (Gibco, Thermo Fisher Scientific, Shanghai, China) supplemented with 10% fetal bovine serum, penicillin (100 IU ml$^{-1}$) and streptomycin (100 μg ml$^{-1}$). The cells were passaged using 0.05% trypsin/0.02% EDTA.

### Mouse models

All animal procedures were performed in accordance with the protocol of Animal Ethics Committee of Shanghai Skin Disease Hospital. The cutaneous SCC mouse model was established using SKH-1 hairless mice purchased from Shanghai public health clinical center (Shanghai, China). SCC XL 50 cells were mixed with 3T3 fibroblast cells with a ratio of 5:1. The SKH-1 hairless mice aged approximate 8 weeks were subcutaneously inoculated with 0.1 ml of cellular mixture ($5 \times 10^5$ XL 50 cells:$1 \times 10^5$ 3T3 fibroblast cells) on the back to form an *in situ* tumor model of SCC [26]. The melanoma mouse model was established using C57BL/6 mice purchased from Shanghai Laboratory Animal Center (Shanghai, China) [27]. Mice, approximately 7 weeks old, were subcutaneously inoculated with 0.1 ml of $6 \times 10^6$ per ml B16F10 cells on the back to form an *in situ* tumor model of skin melanoma.

### In vitro safety assessment

The safety of Cu-Cy NPs *in vitro* was studied using human keratinocyte HaCaT cells. The dark toxicity *in vitro* of Cu-Cy NPs was studied on both SCC XL50 cells and melanoma B16F10 cells. The cell viability was determined by the Cell Counting Kit-8 (CCK-8, Sigma-Aldrich, Shanghai, China) method. HaCaT, XL50 and B16F10 cells ($1 \times 10^4$ per well) were seeded in the 96-well plate and treated by 0.1, 1, 10, 100 or 200 μg/ml of Cu-Cy NPs for 24 h in the dark, respectively. 10 μl of the CCK-8 solution was added to each well. After 2-h incubation, the absorbance at 450 nm for each well was measured using a microplate reader. Each experiment was performed in triplicate and repeated three-times. The cell viability was calculated using the following formula: (optical density value in treated well [−blank])/ (optical density value in control well [−blank]) × 100.

### In vitro effectiveness assessment for cutaneous SCC & melanoma

XL50 cells ($2 \times 10^4$ per well) and B16F10 cells ($2 \times 10^4$ per well) were incubated with 0, 0.1, 1, 10, 100 or 200 μg/ml Cu-Cy NPs in 96-well plates in the dark for 2 h, separately. Cells were irradiated by x-ray (SRT-100™, Sensus Healthcare, FL, USA) at 100 kVp for 150 cGy. After irradiation, the cell medium was changed and cells were incubated for another 24 h to evaluate the cytotoxicity of Cu-Cy NPs using the CCK-8 method. Each experiment was performed in triplicate and repeated three-times.

### In vivo effectiveness assessment for cutaneous SCC & melanoma

To evaluate the effect of Cu-Cy NPs-mediated X-PDT for cutaneous SCC, a total of 20 SCC mice were randomly divided into four groups: X-PDT group, x-ray group, Cu-Cy NPs group and control group (five mice/group). The mice were treated when tumor volume reached 200 mm$^3$. In X-PDT group, 0.1 ml of 0.8 mg/ml Cu-Cy NPs solution was applied to each mouse by multipoint intratumoral injection. After staying in the dark room for 3 h, the mice were irradiated by x-ray (SRT-100, Sensus Healthcare) at 100 kVp with a dose of 200 cGy. In the x-ray

group, 0.9% saline solution was used to replace the Cu-Cy NPs solution. The other procedures were the same as the X-PDT group. In the Cu-Cy NPs group, the mice were intratumorally injected by 0.1 ml of 0.8 mg/ml Cu-Cy NPs solution alone without x-ray irradiation. In the control group, the mice were treated with 0.1 ml 0.9% saline solution alone without x-ray irradiation. After one treatment, mice were observed and tumor volumes were measured every other day. Tumor volumes were calculated using the following formula: $V = (1/2)ab^2$ (a: length, b: width) [40]. Photographs were taken every 5 days. The mice were euthanized by cervical dislocation when the major axis of the tumor grew to over 15 mm.

To evaluate the effect of X-PDT for melanoma, a total of 15 B16F10 melanoma mice were randomly divided into three groups: low dosage X-PDT group, high dosage X-PDT group and control group (five mice/group). The procedures for melanoma mice were largely the same as for SCC mice. After intratumoral injection of Cu-Cy NPs and a light protection for 3 h, mice in the low dosage X-PDT group were irradiated by x-rays at 100 kVp with dose 200 cGy. In the high dosage X-PDT group, the mice were irradiated with dose 400 cGy of x-ray at 100 kVp.

### Evaluation of microvessel density

To evaluate the microvessel density (MVD) after the treatment, tumor tissues of SCC and melanoma were taken from the mice after euthanasia for histopathology and immunohistochemistry examination. Hematoxylin and eosin stain was used for histopathology examination. The expression of CD31, surface marker of neovascular endothelial cells, in tumor tissue was marked by immunohistochemical staining with anti-CD31 antibody (Abcam, Shanghai, China). Images were captured using Leica Application Suite V4.12. The MVD was calculated under a $200\times$ magnification objective lens. For each tumor section, the numbers of CD31 positively stained vessels in top five hotspot fields of view, which showed the greatest density of CD31 positively stained vessels, were counted. MVD was defined as the mean number of CD31 positively stained vessels in these five different hotspot fields of view [11].

### *In vivo* safety assessment

All mice in the study were observed for sudden death or abnormal behavior. One day before mice were euthanized, the food consumption and bodyweight of each mouse were recorded. After the mice were euthanized, the tissue samples of heart, liver, spleen, lung and kidney were taken from the mice in X-PDT and control group for a histopathology examination to assess the safety of Cu-Cy NPs.

### Statistical analyses

Descriptive statistics were obtained using SPSS13.0 software and presented as mean ± standard deviation. The statistical analyses on dark toxicity, cellular survival rates, tumor volumes and MVD were performed using the independent-samples t-test. Mixed-effect linear regression models were used to assess the longitudinal effects of different treatments on tumor volumes while controlling for other factors (time and volume at irradiation), for both cutaneous SCC and melanoma. AR (1) covariance structure as opposed to other structures was preferable based on model selection criteria and was assume in the models to account for the correlated nature of longitudinal data. Tukey's test was used to compare the overall treatment effects between different groups. All regression analyses were conducted in SAS version 9.4 using PROC MIXED. P-value <0.05 was considered statistically significant.

## Results

### Cu-Cy NPs were nontoxic to HaCaT cells without x-ray irradiation

Transmission electron microscope examination showed that Cu-Cy NPs were spherical. The diameter of Cu-Cy NPs was 95.7 ± 8.4 nm (mean ± standard deviation) (Figure 2A). The safety of Cu-Cy NPs *in vitro* was evaluated on HaCaT cells. The survival rates of HaCaT cells are shown in Figure 2B. The results show that Cu-Cy NPs were nontoxic to HaCaT cells without x-ray irradiation in the range of 0.1–200 μg/ml (p > 0.05). The dark toxicity of Cu-Cy NPs was observed in both SCC XL50 cells and melanoma B16F10 cells. When the concentration of Cu-Cy NPs was increased to 200 μg/ml of Cu-Cy NPs, survival rates of both XL50 cells and B16F10 cells were reduced compared with the control group (p < 0.05) (Figure 2B).

### SCC XL50 cells were sensitive to X-PDT while melanoma B16F10 cells were resistant *in vitro*

The cell killing effectiveness of Cu-Cy NPs-mediated X-PDT for cutaneous SCC and melanoma were evaluated separately. The results, shown in Figure 3, show that SCC XL50 cells are more sensitive to the X-PDT than
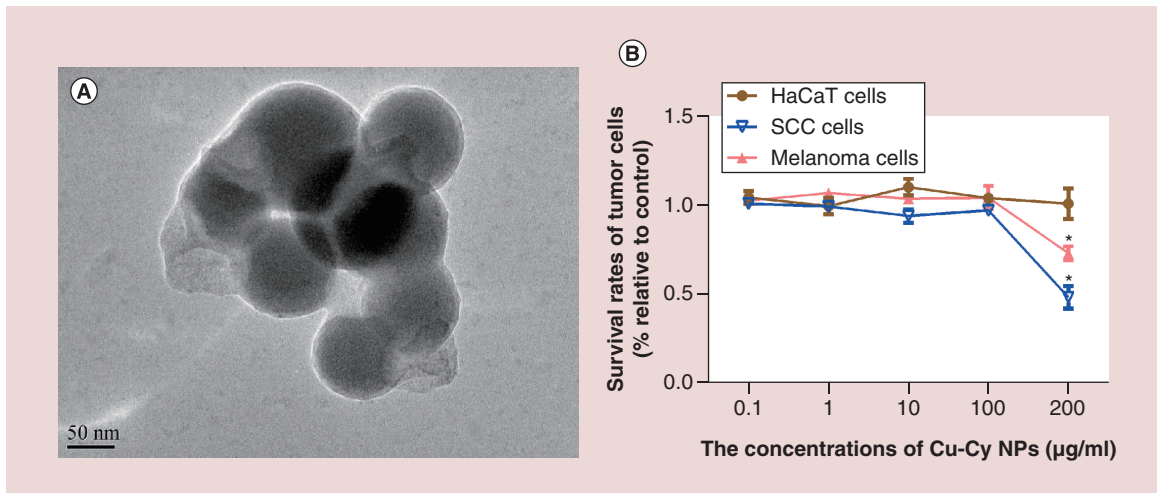
**Figure 2.   Morphology of Copper-cysteamine nanoparticle and its dark toxicity for HaCat, squamous cell carcinoma and melanoma cells. (A)** Copper-cysteamine nanoparticles (Cu-Cy NP) were spherical with a diameter of about 80 nm under transmission electron microscope. **(B)** The survival rates of cells were determined by the CCK-8 method after treated by 0.1, 1, 10, 100 or 200 $\mu$g/ml of Cu-Cy NPs for 24 h *in vitro*. No dark toxicity of Cu-Cy NPs is observed in HaCaT cells. The survival rates of XL50 cells and B16F10 cells were reduced at 200 $\mu$g/ml of Cu-Cy NPs.
*$p < 0.05$ compared with the control group.
Cu-Cy NP: Copper-cysteamine nanoparticles; SCC: Squamous cell carcinoma.
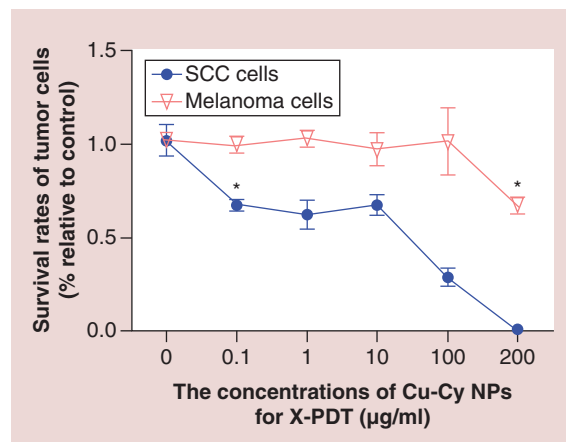


**Figure 3.   Squamous cell carcinoma XL50 cells are more sensitive to x-ray-activated photodynamic therapy compared with melanoma B16F10 cells.** Survival rates of tumor cells were determined by CCK-8 method after treated by 0, 0.1, 1, 10, 100 or 200 $\mu$g/ml of copper-cysteamine nanoparticles-mediated photodynamic therapy under the irradiation of x-rays at 100 kVp with a dose of 150 cGy.
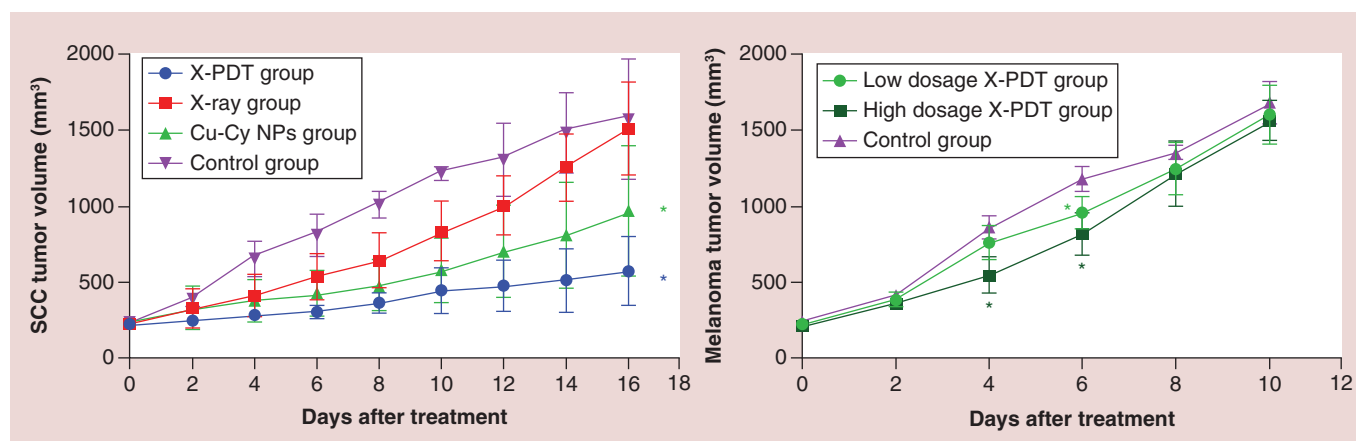*$p < 0.05$ compared with 0 $\mu$g/ml.
Cu-Cy NP: Copper-cysteamine nanoparticle; X-PDT: X-ray-activated photodynamic therapy; SCC: Squamous cell carcinoma.

melanoma B16F10 cells. Only 67.5% SCC cells survive at a Cu-Cy NPs concentration of 0.1 $\mu$g/ml after X-PDT, which is significantly lower than 0 $\mu$g/ml Cu-Cy NPs ($p < 0.05$). And almost 100% of SCC cells are killed at the highest concentration of 200 $\mu$g/ml. However, X-PDT cannot induce melanoma B16F10 cell death at Cu-Cy NPs particle concentrations of 0.1–100 $\mu$g/ml. Only when the concentration reaches 200 $\mu$g/ml, the survival rate (66.8%) is lower than 0 $\mu$g/ml Cu-Cy NPs ($p < 0.05$), implying melanoma B16F10 cells are relatively resistant to X-PDT *in vitro*.

## X-PDT significantly inhibited the growth of SCC *in vivo*

The effectiveness of Cu-Cy NPs-mediated X-PDT for cutaneous SCC *in vivo* was evaluated using tumor volumes shown in Figure 4. Mice were euthanized at day 16 after treatment. Despite all tumor groups growing, the tumors on the mice in the X-PDT group grew much more slowly than other groups. At day 16 after treatment, the tumor volume in the X-PDT group was significantly smaller than the control group and the x-ray group ($p < 0.05$). The tumor volume in the X-PDT group was smaller than Cu-Cy NPs group, but the difference was not statistically significant. The tumor volume in the Cu-Cy NPs group was also smaller than control group ($p < 0.05$), while there was no difference between x-ray group and control group ($p > 0.05$). Representative pictures for the therapeutic

**Figure 4.   X-ray-activated photodynamic therapy successfully inhibited the growth of squamous cell carcinoma while it only temporarily inhibited the growth of B16F10 melanoma.** The tumor volumes of squamous cell carcinoma and melanoma were recorded before and after treatments. X-PDT: copper-cysteamine nanoparticle-mediated x-ray (100 kVp, 200 cGy) activated photodynamic therapy. Low dosage: 200 cGy of irradiation, high dosage: 400 cGy of irradiation.
*p < 0.05 compared with the control group.
Cu-Cy NP: Copper-cysteamine nanoparticle; X-PDT: X-ray activated photodynamic therapy.

**Table 1.  Mixed-effect linear regression models for the longitudinal effects of different treatments on tumor volumes for cutaneous squamous cell carcinoma.**

| Effect | | Estimate | Standard error | t value | Pr > \|t\| | F value | Pr > F |
|---|---|---|---|---|---|---|---|
| | | | | Solution for fixed effects | | | |
| Time | | | | | | 56.75 | <0.0001 |
| | 2 | 0 | – | – | – | | |
| | 4 | 0.1107 | 0.06756 | 1.64 | 0.1038 | | |
| | 6 | 0.1979 | 0.06696 | 2.96 | 0.0037 | | |
| | 8 | 0.3014 | 0.06594 | 4.57 | <0.0001 | | |
| | 10 | 0.4474 | 0.06416 | 6.97 | <0.0001 | | |
| | 12 | 0.5511 | 0.06103 | 9.03 | <0.0001 | | |
| | 14 | 0.6940 | 0.05529 | 12.55 | <0.0001 | | |
| | 16 | 0.8357 | 0.04387 | 19.05 | <0.0001 | | |
| Cu-Cy NPs | | -0.3688 | 0.08301 | | | 19.73 | 0.0005 |
| X-ray | | -0.1834 | 0.08544 | | | 4.61 | 0.0486 |
| Cu-Cy NPs * x-ray | | 0.03859 | 0.1161 | | | 0.11 | 0.7441 |
| Volume at irradiation | | 2.1729 | 1.7740 | | | 1.50 | 0.2395 |

Cu-Cy NP: Copper-cysteamine nanoparticle.

effect are shown in Figure 5. It could also be observed that the growth of tumor in X-PDT group was slower than other groups. At day 15 after treatment, the major axes of the tumors in the control and x-ray groups increased to around 15 mm. Superficial ulcerations arose on the surface of tumors at day 5 after treatment in the control, x-ray and X-PDT groups but not in the Cu-Cy NPs group. The ulcerations grew larger and deeper with time. However, the area and depth of ulceration in X-PDT groups increased more slowly than in the control and x-ray groups (Figure 5). Table 1 shows the results of the mixed-effect linear regression model. Time (p < 0.05) had a positive significant effect on the growth of tumor. However, Cu-Cy NPs (p < 0.05) and x-ray (p < 0.05) had significant negative effects, indicating that both treatments can significantly reduce the tumor volumes. The Tukey's test was further conducted to compare the overall performances between different groups in the whole 16-day treatment period (Table 2). The differences between X-PDT and x-ray (adjusted p < 0.05) are negatively significant, indicating that the X-PDT group performed better than the x-ray group, in terms of reducing the tumor volumes. However, the difference between X-PDT group and Cu-Cy NPs group was not statistically significant.
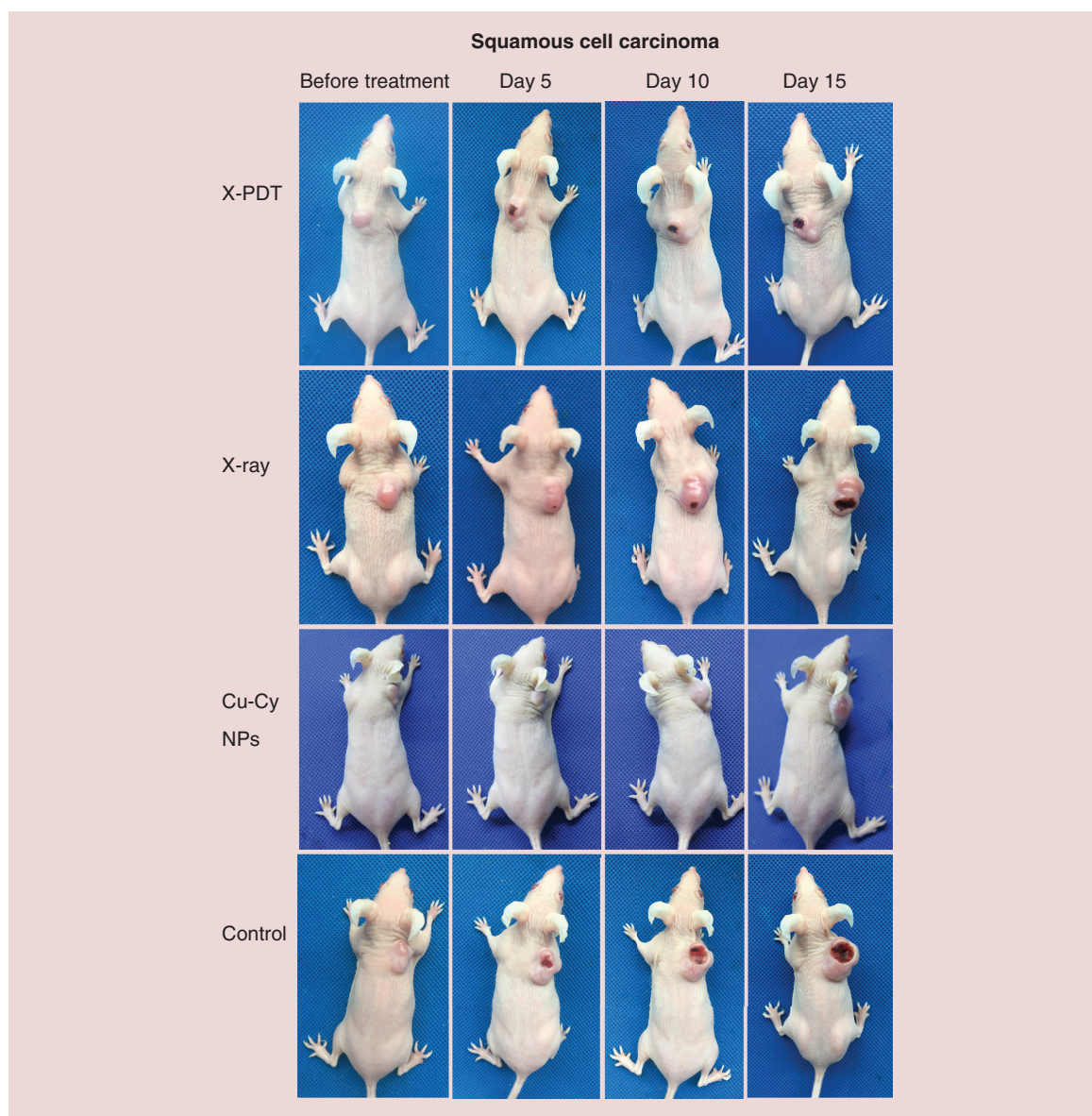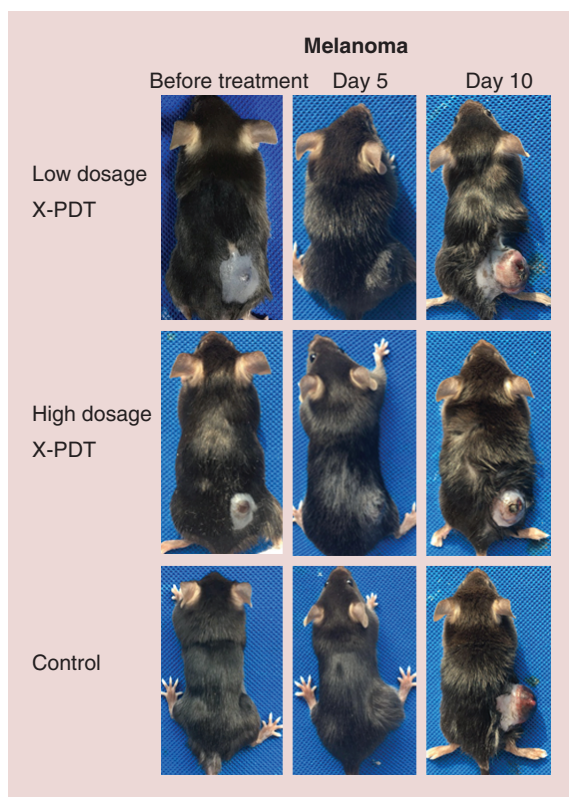
**Figure 5.  Representative photographs of squamous cell carcinoma mice before treatment, at days 5, 10 and 15 after the treatment of copper-cysteamine nanoparticles mediated x-ray-activated photodynamic therapy, x-rays only or copper-cysteamine nanoparticles only.**
Cu-Cy NP: Copper-cysteamine nanoparticle; X-PDT: X-ray activated photodynamic therapy.

**Table 2.  The Tukey's test to compare the overall effectiveness of different treatments for the whole 16-day treatment period.**

| | | Differences of least squares means | | | |
|---|---|---|---|---|---|
| Effect | Estimate | Standard error | t value | Pr > \|t\| | Adj p |
| (X-PDT) – (Cu-Cy NPs) | -0.1448 | 0.08257 | -1.75 | 0.0998 | 0.3321 |
| (X-PDT) – (x-ray) | -0.3302 | 0.08162 | -4.05 | 0.0011 | 0.0052 |
| (X-PDT) – (Control) | -0.5136 | 0.08630 | -5.95 | <.0001 | 0.0001 |
| (Cu-Cy NPs) – (x-ray) | -0.1853 | 0.08219 | -2.26 | 0.0395 | 0.1534 |
| (Cu-Cy NPs) – (Control) | -0.3688 | 0.08301 | -4.44 | 0.0005 | 0.0024 |
| (X-ray) – (Control) | -0.1834 | 0.08544 | -2.15 | 0.0486 | 0.1834 |
| Cu-Cy NP: Copper-cysteamine nanoparticle; X-PDT: X-ray activated photodynamic therapy. | | | | | |

**Figure 6.  Representative photographs of B16F10 melanoma mice before treatment, at days 5 and 10 after the treatment of copper-cysteamine nanoparticles-mediated x-ray-activated photodynamic therapy under low dosage (200 cGy, 100 kVp) or high dosage (400 cGy, 100 kVp) of irradiation.**

In addition, the X-PDT group outperformed the control group (adjusted p = 0.0001) and the Cu-Cy NPs group outperformed the control group (adjusted p = 0.0024). The above results imply X-PDT successfully inhibited the growth of SCC tumors and X-PDT was an effective modality for the treatment of SCC.

### Only high dosage of X-PDT displayed a limited inhibition on B16F10 melanoma *in vivo*

As shown in Figure 4, the experiment ended and mice were euthanized at day 10 after treatment. In all groups, the tumors volumes increased with time. Though there was no difference between each group (p > 0.05) at the end of the experiment, X-PDT slowed down the growth of B16F10 melanoma in the middle of treatment temporarily. The tumor volume in the high-dosage X-PDT group was significantly smaller than the low-dosage X-PDT (p < 0.05) and control groups (p < 0.05) at day 4; and the tumor volume in either high-dosage or low-dosage X-PDT group at day 6 was smaller than control group (p < 0.05). The representative pictures show the major axis of the tumors in all groups was longer than 15 mm and erosion or ulceration arose on the surface of the B16F10 melanoma at day 10 after treatment (Figure 6). Results of the mixed-effect linear regression model are shown in Table 3. As for SCC, time (p < 0.05) also had a significant positive effect on the growth of tumor. However, the dosage of x-ray for X-PDT (p < 0.05) had a negative effect on the growth of B16F10 melanoma. Table 4 shows the results of the Tukey's test for the whole 10-day treatment period. We observed that the low-dosage X-PDT group was not significantly different from the control group (adjusted p > 0.05); the low-dosage X-PDT group was not significantly different from the high-dosage group (adjusted p > 0.05); and the high-dosage X-PDT group was significantly better than the control group (adjusted p < 0.05), in terms of overall treatment effects. The above results indicate B16F10 melanoma is resistant to X-PDT. The effect of X-PDT was temporary. If considering overall effect, only high dosage of X-PDT displayed an inhibition on B16F10 melanoma in a certain degree.

### X-PDT induced an inhibition of vascularization in SCC

The results of histopathology and immunohistochemistry (Figure 7) show the tumor vessels and CD31 expression (brown staining) of SCC tissue in X-PDT, x-ray and Cu-Cy NPs group was obviously less than control group. For B16F10 melanoma, the images (Figure 8) show that there was no apparent difference in the tumor vessels and CD31 expression between each group. The results of MVD stained by anti-CD31 antibody is shown in Figure 9.

**Table 3. Mixed-effect linear regression models for the longitudinal effects of different treatments on tumor volumes for B16F10 melanoma.**

| | | Solution for fixed effects | | | | | |
|---|---|---|---|---|---|---|---|
| Effect | | Estimate | Standard error | t value | Pr > \|t\| | F value | Pr > F |
| Time | | | | | | 362.90 | <0.0001 |
| | 2 | 0 | – | – | – | | |
| | 4 | 0.3370 | 0.04247 | 7.94 | <0.0001 | | |
| | 6 | 0.6023 | 0.04167 | 14.45 | <0.0001 | | |
| | 8 | 0.8904 | 0.03956 | 22.51 | <0.0001 | | |
| | 10 | 1.2382 | 0.03355 | 36.90 | <0.0001 | | |
| Dosage | | | | | | 8.58 | 0.0057 |
| | Control | 0 | – | – | – | | |
| | Low | -0.1161 | 0.04820 | -2.41 | 0.0348 | | |
| | High | -0.2282 | 0.05509 | -4.14 | 0.0016 | | |
| Volume at irradiation | | -1.0578 | 1.1397 | | | 0.86 | 0.3733 |

**Table 4. The Tukey's test to compare the overall effectiveness of different treatments for the whole 10-day treatment period.**

| | Differences of least squares means | | | | |
|---|---|---|---|---|---|
| Effect | Estimate | Standard error | t value | Pr > \|t\| | Adj p |
| (Low) – (High) | 0.1122 | 0.04707 | 2.38 | 0.0363 | 0.0853 |
| (Low) – (Control) | -0.1161 | 0.04820 | -2.41 | 0.0348 | 0.0819 |
| (High) – (Control) | -0.2282 | 0.05509 | -4.14 | 0.0016 | 0.0043 |
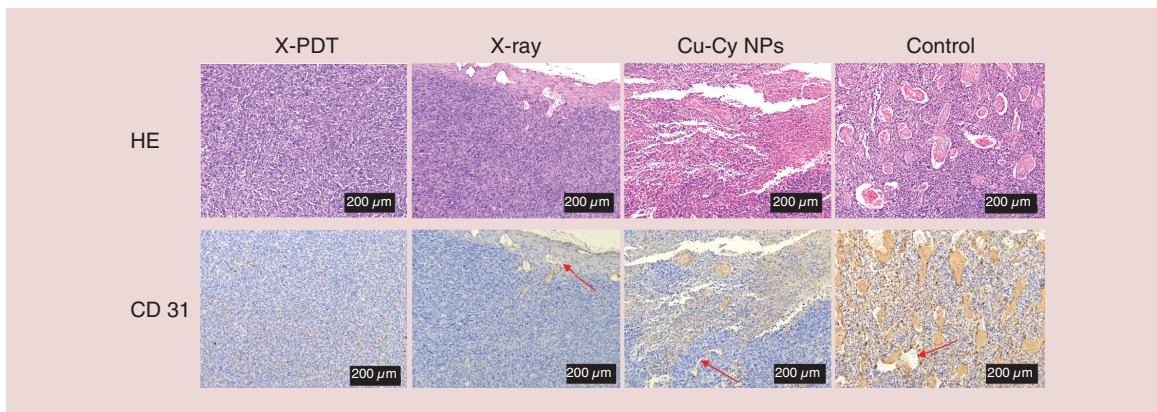


**Figure 7. X-ray-activated photodynamic therapy induced the inhibition of vascularization in squamous cell carcinoma tissue.** Histopathology examination stained by hematoxylin and eosin and immunohistochemistry examination stained by anti-CD31 antibody were used to assess the tumor vessels in squamous cell carcinoma tissue at day 16 after the treatments. CD31 positively stained tumor vessels in x-ray-activated photodynamic therapy (X-PDT), x-ray and copper-cysteamine nanoparticles groups were obviously less than control. Especially, there was nearly no tumor vessels observed in X-PDT group.
Cu-Cy NP: Copper-cysteamine nanoparticle; HE: Hematoxylin and eosin; X-PDT: X-ray-activated photodynamic therapy.

MVD of SCC tissue in X-PDT, x-ray, and Cu-Cy NPs group was significantly lower than control group ($p < 0.05$). Among them, X-PDT group showed the lowest value of MVD, which implied that X-PDT displayed the strongest inhibition of vascularization in SCC tissue. For B16F10 melanoma, there was no significant difference in the number of CD31 positively stained tumor vessels (Figures 8 & 9) between each group.
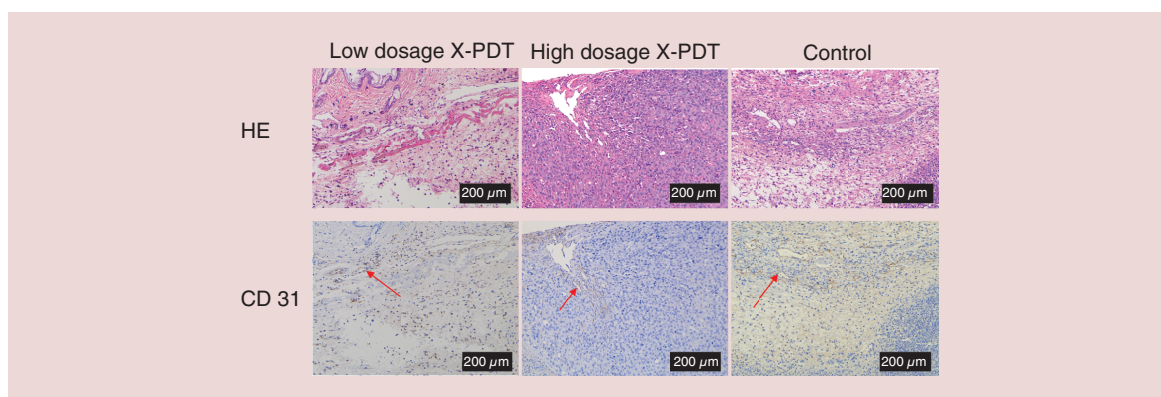
**Figure 8.   No apparent inhibition of vascularization caused by x-ray-activated photodynamic therapy was observed in B16F10 melanoma tissue.** Histopathology examination stained by hematoxylin and eosin and immunohistochemistry examination stained by anti-CD31 antibody were used to assess the tumor vessels in melanoma tissue at day 10 after the treatments. The number of CD31 positively stained tumor vessels in the control group was similar to the low-dosage x-ray-activated photodynamic therapy (X-PDT) and high-dosage X-PDT groups. HE: Hematoxylin and eosin; X-PDT: X-ray-activated photodynamic therapy.
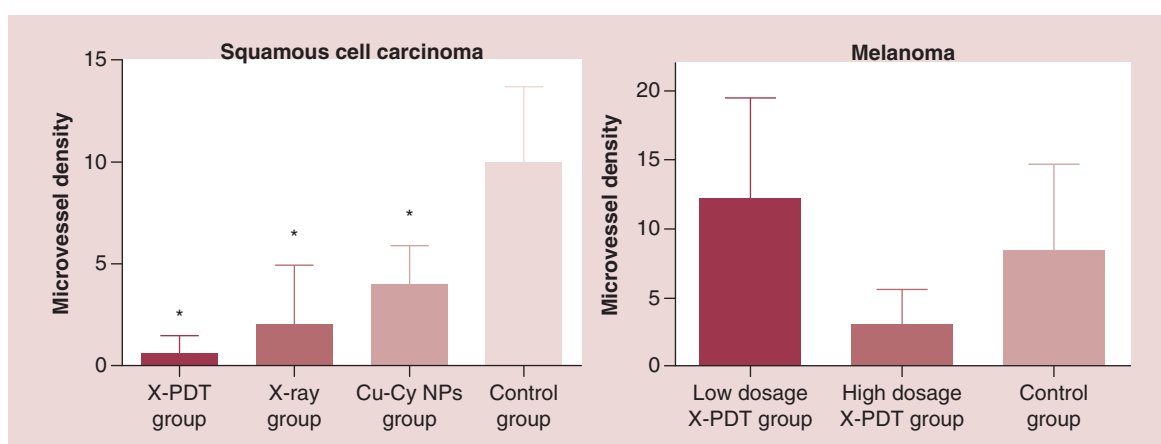


**Figure 9.   X-ray-activated photodynamic therapy reduced the microvessel density in squamous cell carcinoma tissue significantly.** A high-dosage x-ray-activated photodynamic therapy (X-PDT) with an irradiation of 400 cGy reduced the microvessel density in B16F10 melanoma tissue but no significant difference.
*p < 0.05 compared with the control group.
Cu-CyNP: Copper-cysteamine nanoparticle; MVD: Microvessel density; X-PDT: X-ray-activated photodynamic therapy.

### *In vivo* safety assessment

The safety of Cu-Cy NPs *in vivo* was evaluated on both SCC mice and melanoma mice. During the observation period, no mice died or showed abnormal behavior. At the end of treatment, there was no significant change of food consumption (p > 0.05) or bodyweight (p > 0.05) between treatment groups and the control group (Figure 10). Histopathology examination for the heart, liver, spleen, lung and kidney did not show any metastatic tumor cell, inflammation or necrosis (Figures 11 & 12). The results suggest that no organ damage occurred in this topical X-PDT treatment. Generally, no obvious acute toxicity reaction observed in the study.

### Discussion

Treatments for cutaneous SCC and melanoma are still big challenges in the clinic. PDT is a less invasive treatment composed of targeted ablation and immune activation. Based on its good effect and minor adverse reactions, PDT has been widely used in the treatments for various cancers. It was successfully applied to treat superficial cutaneous SCC in the clinic. However, the effectiveness of PDT for the deep cutaneous SCC or melanoma remains inconclusive. X-PDT is a potentially effective treatment for deep tumor and melanoma. X-rays are able to penetrate
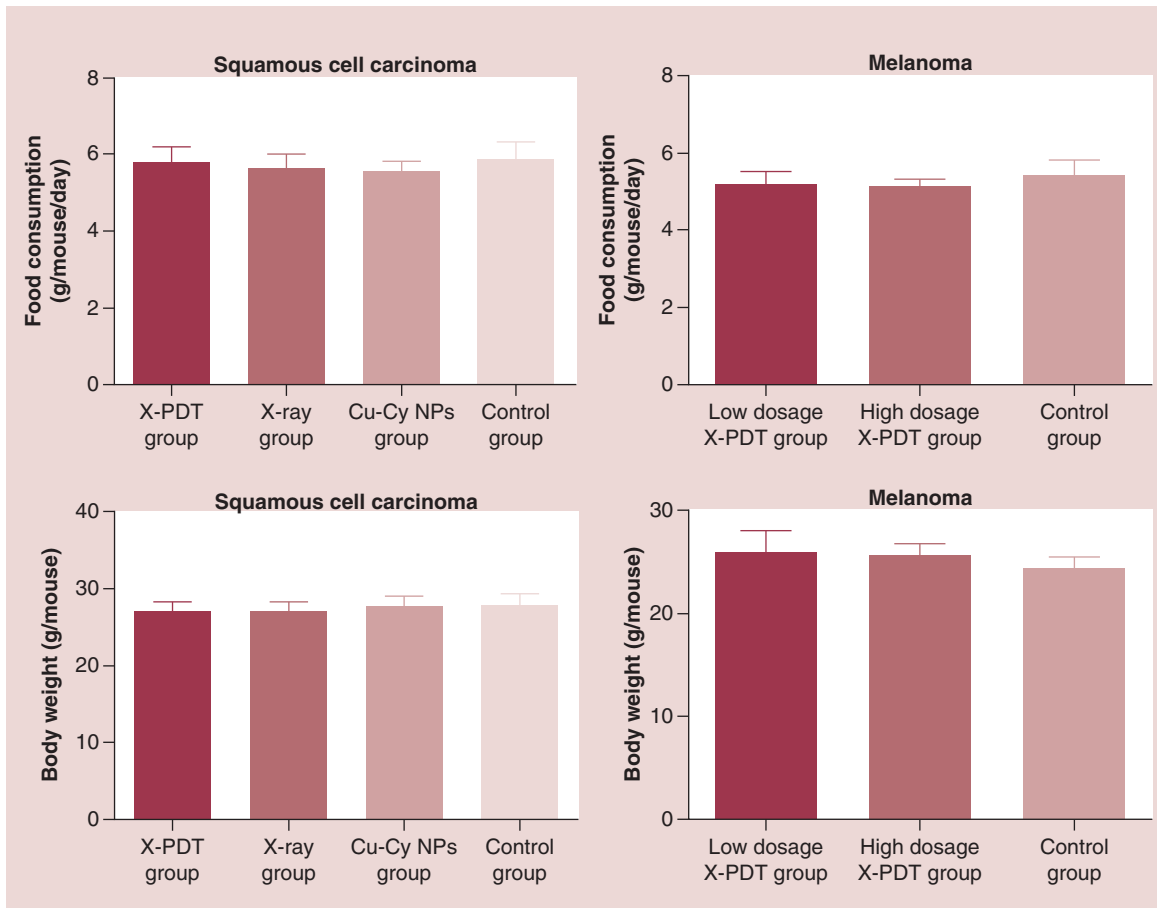
**Figure 10.   The food consumption and bodyweight of each mouse were recorded 1 day before mice were euthanized.** There is no significant change of food consumption (p > 0.05) or bodyweight between treatment groups and the control group (p > 0.05).
Cu-Cy NP: Copper-cysteamine nanoparticle; X-PDT: X-ray-activated photodynamic therapy.
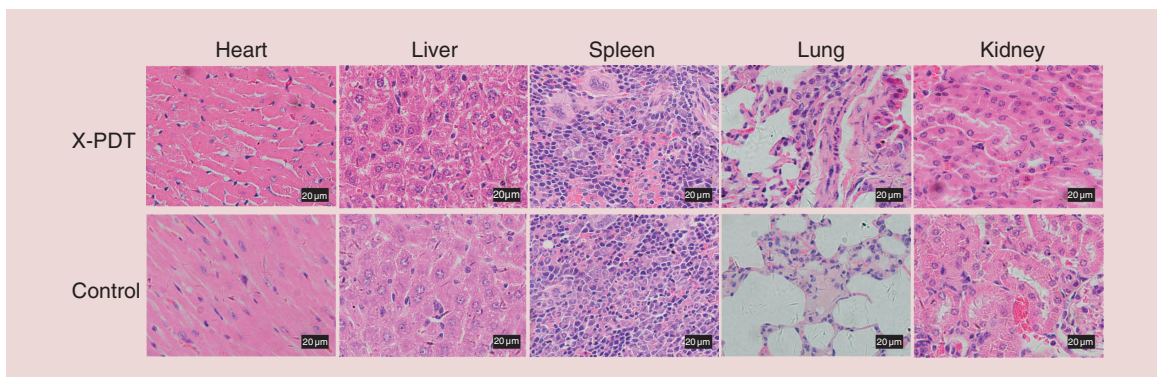


**Figure 11.   Histopathologic examination of the tissues from the heart, liver, spleen, lung and kidney of the squamous cell carcinoma mice in the x-ray-activated photodynamic therapy group and the control group.** No metastatic tumor cell, inflammation or necrosis was seen in these organs.
X-PDT: X-ray-activated photodynamic therapy.
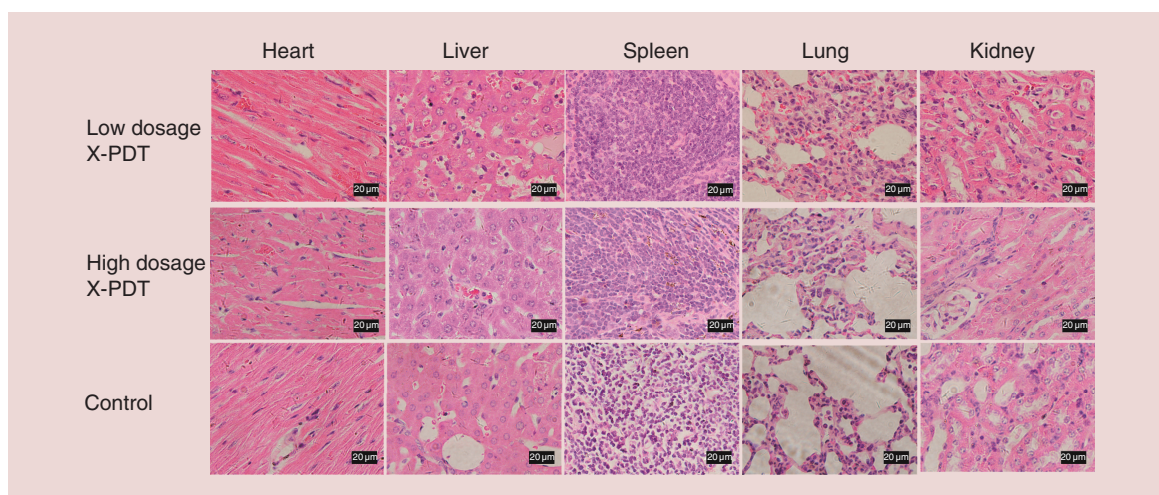
**Figure 12.   Histopathologic examination of the tissues from the heart, liver, spleen, lung and kidney of B16F10 melanoma mice in the low-dosage (200 cGy, 100 kVp), high-dosage (400 cGy, 100 kVp) x-ray-activated photodynamic therapy group and the control group.** No metastatic tumor cell, inflammation or necrosis was seen in these organs. X-PDT: X-ray-activated photodynamic therapy.

into the deep skin and activate the photodynamic effect in tumor tissues. Both the photodynamic effect and the ionizing irradiation induced by x-rays exert the antitumor effect at the same space and time to override tumor cell repairs (Figure 1) [28].

Cu-Cy NPs were first prepared and reported by Chen and colleagues in 2014 [22]. Cu-Cy NPs used in this study had a diameter of 95.7 ± 8.4 nm (mean ± standard deviation) (Figure 2A). The nanoparticles of around this size usually showed a collective advantage of deep tumor tissue penetration and efficient cancer cell internalization as well as slow tumor clearance, resulting in a strong tumor-suppressing activity [29,30]. It was demonstrated that Cu-Cy NPs could generate plentiful singlet oxygen under x-ray irradiation [22,24,31]. Beside x-rays, ultraviolet light [22], microwave [32] and ultrasound [33] can also excite Cu-Cy NPs to produce singlet oxygen, hydroxyl radicals and other ROS to inhibit the growth of tumors. Even when in an acidic environment, Cu-Cy NPs can release copper ions and accelerate the production of ROS in biological systems without light [34–37]. Copper ions as a reactive metal can convert oxygen to hydrogen peroxide ($H_2O_2$). Then, $H_2O_2$ can further generate singlet oxygen via disproportionation [34,35,37]. In the absence of any above activating factors, Cu-Cy NPs alone were nontoxic to nontumorous keratinocyte HaCaT cells in the range of 0.1–200 μg/ml *in vitro*. For SCC XL 50 cells and melanoma B16F10 cells, there is no dark toxicity of Cu-Cy NPs in the range of 0.1–100 μg/ml *in vitro*. However, Cu-Cy NPs alone showed the dark toxicity to XL50 cells and B16F10 cells when the concentration increased to 200 μg/ml (Figure 2B). Therefore, we did not increase the concentration of the Cu-Cy NPs beyond 200 μg/ml in this study. The results of *in vitro* effectiveness assessment of X-PDT showed even a lowest concentration of 0.1 μg/ml of Cu-Cy NPs-mediated X-PDT could induce a significant inhibition of the proliferation of SCC XL50 cells indicating that Cu-Cy NPs were activated to induce the photodynamic response under the irradiation of x-ray (Figure 3). In the *in vivo* study, although X-PDT did not completely eliminate the tumor, it still significantly inhibited the growth of SCC (Figures 4, 5 & Tables 1, 2). In addition, it was found that time had a positive effect on the growth of tumor (Table 1), which implies that a better result might be achieved if SCC had been treated earlier. In this study, X-PDT was performed only one time. In the clinic, several times of PDT are needed to eliminate even superficial SCC. The effectiveness of X-PDT would be further improved if it was repeated. The interesting result was that Cu-Cy NPs alone also inhibited the growth of SCC on the mice (Figures 4, 5 & Tables 1, 2) [22,24]. This might be because the acidic environment inside the tumor tissue induced the release of copper ions from Cu-Cy NPs. Copper ions contribute to the production of $H_2O_2$ and singlet oxygen as mentioned above. Though tumor volume in the X-PDT group was smaller than Cu-Cy NPs group, there was no statistically significant difference between the two groups. This could be because the x-ray irradiation was used in a low dosage and for only one time in the study. In addition, ulcerations arose on the surface of SCC in the control, x-ray and X-PDT groups (Figure 5). The ulceration occurred on the tumor because the fast growth of tumor outstrips its blood supply, leading to the tumor

necrosis [38]. The ulceration in the x-ray group grew as fast as the control group mostly because x-ray treatment could not significantly inhibit the growth of SCC. Although the growth of SCC was significantly inhibited in both the X-PDT group and the Cu-Cy NPs group, a small and relatively superficial ulceration occurred only on the tumor in the X-PDT group. On the one hand, X-PDT significantly inhibited tumor angiogenesis, which largely reduced the blood supply of tumor resulting in the necrosis of tumor. On the other hand, x-rays also damaged the surrounding normal cells, such as the keratinocytes and fibroblasts, which caused ulceration and hindered the healing of ulcerations [39]. The above results imply that ulceration should be monitored when X-PDT is used for SCC, to avoid massive hemorrhage or excessive destruction on special sites.

In this study, B16F10 melanoma was found to be resistant to X-PDT in both *in vitro* and *in vivo*. *In vitro*, the survival rate of melanoma B16F10 cells was reduced only at a highest concentration of 200 μg/ml of Cu-Cy NPs (Figure 3). *In vivo*, only at the early stage of treatment, X-PDT slowed down the growth of B16F10 melanoma temporally (Figures 4 & 6). There was no difference of volumes in different groups at the end of treatment, although the high-dosage X-PDT group showed a significant overall treatment effect if using the Tukey's test to compare the volumes in the whole 10-day treatment period (Table 4). In generally, antitumor efficacy of X-PDT in B16F10 melanoma was unsatisfied in this study. As shown in the analysis summarized in Table 3, time had a positive effect while the dosage of x-ray for X-PDT had a negative effect on the growth of B16F10 melanoma indicating an earlier treatment or a higher dosage of x-ray irradiation might improve the effectiveness of X-PDT on melanoma. However, due to the high mortality rate of melanoma, surgery is usually the first choice for early-stage melanoma [40]. For mouse experiments in the study, even a 400 cGy of high-dosage x-ray irradiation could not remarkably inhibit the growth of B16F10 melanoma for a long time. A higher dosage of modality of x-ray irradiation would be hard to applied because of the side effects of x-ray [41]. There seems to be no room for the potential application of a higher dosage of X-PDT for melanoma. In addition, it is well known that melanoma is insensitive to either x-ray radiation therapy or PDT [10,42]. The mechanism of its radio-resistance is linked to the overexpression of tyrosinase-related protein 2 in melanoma cells [43]. The mechanisms of its PDT-resistance include optical interference, antioxidant defense of melanin and cytoprotective response through the induction of autophagy of melanoma cells [44–46]. Melanin plays an important role in resistance of melanoma to PDT. It may act as a filter to prevent any in-depth penetration of light, shielding certain cellular targets from light and also may act as a ROS scavenger decreasing high levels of ROS [44,47].

The histopathology and immunohistochemistry examinations showed that the vascularization inside the SCC tissue were inhibited by X-PDT and tumor vessels became less most apparently (Figure 7). MVD in SCC tissue was significantly reduced by x-ray, Cu-Cy NPs and X-PDT (Figure 9). It is demonstrated that x-rays can damage or kill tumor vascular endothelial cells, inducing a denudation of the tumor vascular endothelium, which causes a decrease in number of vessels, leading to a decrease in perfusion and to tumor hypoxia [48]. In addition, it is reported that the endothelial cells from tumor tissue are significantly more radiosensitive than the endothelial cells from normal tissue [49]. As we known, the effect of tumor vessels is also a main mechanism of PDT for antitumor treatments [50,51]. In this study, Cu-Cy NPs alone might induce the reduction of MVD through the photodynamic response activated by the acidic environment inside SCC. X-PDT showed the most apparent inhibition of vascularization in SCC tissue because of simultaneous or even synergistic effect of x-ray and PDT on tumor vascular endothelium. The damage of tumor vascular endothelium by X-PDT mightily promoted the release of thromboxane and nitric oxide, which further resulted in vessel constriction, collapse and blocking [52,53]. The collapse of vessels inside tumors contributes to the long-term tumor control by the deprivation of oxygen and nutrients in the tumor and consequent tumor infarction [51,54]. However, for B16F10 melanoma, no apparent inhibition of vascularization was observed (Figures 8 & 9), indicating the vascular endothelium in B16F10 melanoma is resistant to X-PDT. Based on the strong effect on tumor vessels in SCC induced a strong inhibition on the growth of SCC, it was concluded that a stronger vascular effect could induce a more effective tumor response to PDT [5]. In intravenous PDT, short drug-light interval (15 min – 2 h) allows for more photosensitizers to accumulate in the tumor vascular endothelial cells and causes stronger suppressions of tumor growth than long drug-light interval (3–6 h), indicating that the damage of vascular endothelial cells plays an important role in the inhibition of tumors in these studies [55–58]. Furthermore, the vascular effect by PDT could be used to enhance the effectiveness of other therapies on tumors. In the early stage of vessel damage, the contraction of endothelial cells caused by PDT increases tumor vessel leakiness; this leakiness augments the enhanced permeability retention effect of nanometer-scale antitumor drugs [59]. In the advanced stage of vessel damage, tumor vessels collapsed and blocked, leading to a decrease in the interstitial fluid pressure inside tumors. The low interstitial fluid pressure facilitated the convection of an antitumor chemical drug

inside the tumor tissue from the intravascular to extravascular side, enhancing the homogeneous distribution or effective permeability of an antitumor drug in tumor tissue [60]. Therefore, the vascular effect caused by PDT plays an important role in an antitumor treatment. In addition, the vascular effect caused by PDT is normally limited to the tumor tissue, leaving normal tissue unaffected, because of the high proliferative capacity of cancerous vascular endothelial cells [61].

The results for safety showed that Cu-Cy NPs alone were nontoxic to HaCaT cells *in vitro*. No acute toxicity reaction occurred after the X-PDT *in vivo*, such as sudden death, abnormal behavior, significant changes of food consumption, significant changes in bodyweight (Figure 10) or damages observed in the heart, liver, spleen, lung and kidney of mice (Figures 11 & 12). Because skin cancers are usually limited in local skin, topical PDT is more suitable approach than intravenous PDT for the treatment of skin cancers [1]. Considering the concerns about the potentially toxicity of nanoparticles, the use of topical administration might diminish the potential systematic damage caused by nano-photosensitizers. Therefore, topical PDT for skin cancers might be a pioneering advance to transfer the nanotechnology to the clinic.

## Conclusion

Cu-Cy NPs-mediated X-PDT is a safe modality for skin cancers. *In vitro*, it exhibited a strong cytotoxicity to SCC cells. *In vivo*, it induced a strong inhibition of vascularization and successfully suppressed the growth of SCC. However, B16F10 melanoma was resistant to X-PDT both *in vitro* and *in vivo*.

## Future perspective

Based on its feasibility, effectiveness and safety, topical X-PDT might be an optional therapy for cutaneous SCC in the clinic in the future. Before the clinical transformation, the safety of nanoparticles for human being, the effect of immune activation of X-PDT need to be further clarified. Once X-PDT is transformed to the clinic, it also can be applied to the treatment of other cancers, such as nasopharynx cancer, bladder cancer, breast cancer, osteosarcoma and so on. For melanoma, the combination of X-PDT with immune checkpoint therapy might become a research hotspot in the future.

---

### Summary points

- Copper-cysteamine nanoparticles (Cu-Cy NPs) were nontoxic for human keratinocyte cells without the x-ray irradiation.
- Squamous cell carcinoma (SCC) XL50 cells are sensitive to the treatment of Cu-Cy NPs-mediated x-ray-activated photodynamic therapy (X-PDT) *in vitro*.
- Melanoma B16F10 cells are resistant to the X-PDT *in vitro*.
- X-PDT successfully inhibited the growth of SCC significantly *in vivo* ($p < 0.05$).
- The vascularization inside SCC was inhibited by X-PDT and the expression of CD31 and the microvessel density were reduced indicating that tumor angiogenesis was inhibited by X-PDT.
- For B16F10 melanoma, X-PDT did not decrease the microvessel density of melanoma significantly and only slowed down the growth of melanoma temporary at the early stage of the treatment ($p < 0.05$).
- No obvious acute toxicity reaction was observed in the study.

### Ethical conduct of research

All animal procedures were performed in accordance with the protocol of Animal Ethics Committee of Shanghai Skin Disease Hospital. The authors state that they have obtained appropriate institutional review board approval or have followed the principles outlined in the Declaration of Helsinki for all human or animal experimental investigations.

## References

Papers of special note have been highlighted as: • of interest; •• of considerable interest

1.  Wang XL, Wang HW, Guo MX, Xu SZ. Treatment of skin cancer and pre-cancer using topical ALA-PDT–a single hospital experience. *Photodiagnosis Photodyn. Ther.* 5(2), 127–133 (2008).

2.  Castano AP, Mroz P, Hamblin MR. Photodynamic therapy and anti-tumour immunity. *Nat. Rev. Cancer* 6(7), 535–545 (2006).

3.  Wang X, Ji J, Zhang H *et al.* Stimulation of dendritic cells by DAMPs in ALA-PDT treated SCC tumor cells. *Oncotarget* 6(42), 44688–44702 (2015).

4.  Li Z, Agharkar P, Chen B. Therapeutic enhancement of vascular-targeted photodynamic therapy by inhibiting proteasomal function. *Cancer Lett.* 339(1), 128–134 (2013).

5.  Maas AL, Carter SL, Wileyto EP *et al.* Tumor vascular microenvironment determines responsiveness to photodynamic therapy. *Cancer Res.* 72(8), 2079–2088 (2012).

6.  Kawczyk-Krupka A, Wawrzyniec K, Musiol SK, Potempa M, Bugaj AM, Sieron A. Treatment of localized prostate cancer using WST-09 and WST-11 mediated vascular targeted photodynamic therapy-A review. *Photodiagnosis Photodyn. Ther.* 12(4), 567–574 (2015).

7.  Clement S, Chen W, Deng W, Goldys EM. X-ray radiation-induced and targeted photodynamic therapy with folic acid-conjugated biodegradable nanoconstructs. *Int. J. Nanomedicine* 13, 3553–3570 (2018).

8.  Wang C, Tao H, Cheng L, Liu Z. Near-infrared light induced *in vivo* photodynamic therapy of cancer based on upconversion nanoparticles. *Biomaterials* 32(26), 6145–6154 (2011).

9.  Siemann DW. The unique characteristics of tumor vasculature and preclinical evidence for its selective disruption by tumor-vascular disrupting agents. *Cancer Treat. Rev.* 37(1), 63–74 (2011).

10. Huang YY, Vecchio D, Avci P, Yin R, Garcia-Diaz M, Hamblin MR. Melanoma resistance to photodynamic therapy: new insights. *Biol. Chem.* 394(2), 239–250 (2013).

11. Miyata Y, Mitsunari K, Asai A, Takehara K, Mochizuki Y, Sakai H. Pathological significance and prognostic role of microvessel density, evaluated using CD31, CD34, and CD105 in prostate cancer patients after radical prostatectomy with neoadjuvant therapy. *Prostate* 75(1), 84–91 (2015).

12. Kamkaew A, Chen F, Zhan Y, Majewski RL, Cai W. scintillating nanoparticles as energy mediators for enhanced photodynamic therapy. *ACS Nano* 10(4), 3918–3935 (2016).

13. Cline B, Delahunty I, Xie J. Nanoparticles to mediate x-ray-induced photodynamic therapy and Cherenkov radiation photodynamic therapy. *Wiley Interdiscip. Rev. Nanomed. Nanobiotechnol.* 11(2), e1541 (2018).

14. Popovich K, Tomanova K, Cuba V *et al.* LuAG:Pr$^{3+}$-porphyrin based nanohybrid system for singlet oxygen production: toward the next generation of PDTX drugs. *J. Photochem. Photobiol. B.* 179, 149–155 (2018).

15. Zou X, Yao M, Ma L *et al.* X-ray-induced nanoparticle-based photodynamic therapy of cancer. *Nanomedicine (Lond).* 9(15), 2339–2351 (2014).

16. Chen W, Zhang J. Using nanoparticles to enable simultaneous radiation and photodynamic therapies for cancer treatment. *J. Nanosci. Nanotechnol.* 6(4), 1159–1166 (2006).

17. Chen H, Wang GD, Chuang YJ *et al.* Nanoscintillator-mediated x-ray inducible photodynamic therapy for *in vivo* cancer treatment. *Nano Lett.* 15(4), 2249–2256 (2015).

18. Hu J, Tang Y, Elmenoufy AH, Xu H, Cheng Z, Yang X. Nanocomposite-based photodynamic therapy strategies for deep tumor treatment. *Small* 11(44), 5860–5887 (2015).

19. Larue L, Ben Mihoub A, Youssef Z *et al.* Using x-rays in photodynamic therapy: an overview. *Photochem. Photobiol. Sci.* 17(11), 1612–1650 (2018).

20. Shi L, Wang X, Zhao F *et al.* In vitro evaluation of 5-aminolevulinic acid (ALA) loaded PLGA nanoparticles. *Int. J. Nanomedicine* 8, 2669–2676 (2013).

21. Wang X, Shi L, Tu Q *et al.* Treating cutaneous squamous cell carcinoma using 5-aminolevulinic acid polylactic-co-glycolic acid nanoparticle-mediated photodynamic therapy in a mouse model. *Int. J. Nanomedicine* 10, 347–355 (2015).

22. Ma L, Zou X, Chen W. A new x-ray activated nanoparticle photosensitizer for cancer treatment. *J. Biomed. Nanotechnol.* 10(8), 1501–1508 (2014).

•• **This research demonstrated the copper-cysteamine nanoparticles (Cu-Cy NPs) could produce singlet oxygen under the irradiation of x-ray or UV light.**

23.  Akafzade H, Sharma SC, Hozhabri N, Chen W, Ma L. Raman spectroscopy analysis of new copper-cysteamine photosensitizer. *J. Raman Spectrosc.* 50(4), 522–527 (2019).

24.  Liu Z, Xiong L, Ouyang G *et al.* investigation of copper cysteamine nanoparticles as a new type of radiosensitiers for colorectal carcinoma treatment. *Sci. Rep.* 7(1), 9290 (2017).

25.  Huang X, Wan F, Ma L *et al.* Investigation of copper-cysteamine nanoparticles as a new photosensitizer for anti-hepatocellular carcinoma. *Cancer Biol. Ther.* 20(6), 812–815 (2019).

26.  Keyal U, Luo Q, Bhatta AK *et al.* Zinc pthalocyanine-loaded chitosan/mPEG-PLA nanoparticles-mediated photodynamic therapy for the treatment of cutaneous squamous cell carcinoma. *J. Biophotonics* 11(11), e201800114 (2018).

27.  Mead MJ, Nathanson SD, Lee M, Peterson E. Prophylactic lymphadenectomy for B16 melanoma in C57/BL6 mice: survival based on size and heterogeneous variant of the primary. *J. Surg. Res.* 38(4), 319–327 (1985).

28.  Wang GD, Nguyen HT, Chen H *et al.* X-ray induced photodynamic therapy: a combination of radiotherapy and photodynamic therapy. *Theranostics* 6(13), 2295–2305 (2016).

29.  Bao H, Zhang Q, Xu H, Yan Z. Effects of nanoparticle size on antitumor activity of 10-hydroxycamptothecin-conjugated gold nanoparticles: *in vitro* and *in vivo* studies. *Int. J. Nanomedicine* 11, 929–940 (2016).

30.  Tang L, Yang X, Yin Q *et al.* Investigating the optimal size of anticancer nanomedicine. *Proc. Natl Acad. Sci. USA* 111(43), 15344–15349 (2014).

31.  Ma L, Chen W, Schatte G *et al.* A new Cu-cysteamine complex: structure and optical properties. *J. Mater. Chem. C.* 2, 4239–4246 (2014).

32.  Yao M, Ma L, Li L *et al.* A new modality for cancer treatment–nanoparticle mediated microwave induced photodynamic therapy. *J. Biomed. Nanotechnol.* 12(10), 1835–1851 (2016).

•    **This research demonstrated the Cu-Cy NPs could produce singlet oxygen under the irradiation of microwave.**

33.  Wang P, Wang X, Ma L *et al.* Nanosonosensitization by using copper–cysteamine nanoparticles augmented sonodynamic cancer treatment. *Part. Part. Syst. Charact.* 35, 1700378 (2018).

•    **This research demonstrated Cu-Cy NPs could produce reactive oxygen species upon the exposure to ultrasound.**

34.  Lee EC, Ha E, Singh S *et al.* Copper(II)-human amylin complex protects pancreatic cells from amylin toxicity. *Phys. Chem. Chem. Phys.* 15(30), 12558–12571 (2013).

35.  Wang C, Liu L, Zhang L, Peng Y, Zhou F. Redox reactions of the alpha-synuclein-$Cu^{2+}$ complex and their effects on neuronal cell viability. *Biochemistry* 49(37), 8134–8142 (2010).

36.  Hewitt N, Rauk A. Mechanism of hydrogen peroxide production by copper-bound amyloid beta peptide: a theoretical study. *J. Phys. Chem. B.* 113(4), 1202–1209 (2009).

37.  Yao M, Ma L, Li L *et al.* A new modality for cancer treatment–nanoparticle mediated microwave induced photodynamic therapy. *J. Biomed. Nanotechnol.* 12(10), 1835–1851 (2016).

38.  Nthumba PM. Squamous cell carcinoma (Marjolin's ulcer) in an orocutaneous fistula of a large mandibular ameloblastoma: a case report. *J. Med. Case Rep.* 5, 396 (2011).

39.  Iyer S, Balasubramanian D. Management of radiation wounds. *Indian J. Plast. Surg.* 45(2), 325–331 (2012).

40.  Berrocal A, Arance A, Castellon VE *et al.* SEOM clinical guideline for the management of malignant melanoma (2017). *Clin. Transl. Oncol.* 20(1), 69–74 (2018).

41.  Bonomo P, Loi M, Desideri I *et al.* Incidence of skin toxicity in squamous cell carcinoma of the head and neck treated with radiotherapy and cetuximab: A systematic review. *Crit. Rev. Oncol. Hematol.* 120, 98–110 (2017).

42.  Mahadevan A, Patel VL, Dagoglu N. Radiation therapy in the management of malignant melanoma. *Oncology (Williston Park).* 29(10), 743–751 (2015).

43.  Pak BJ, Lee J, Thai BL *et al.* Radiation resistance of human melanoma analysed by retroviral insertional mutagenesis reveals a possible role for dopachrome tautomerase. *Oncogene* 23(1), 30–38 (2004).

44.  Hadjur C, Richard MJ, Parat MO, Jardon P, Favier A. Photodynamic effects of hypericin on lipid peroxidation and antioxidant status in melanoma cells. *Photochem. Photobiol.* 64(2), 375–381 (1996).

45.  Busetti A, Soncin M, Jori G, Rodgers MA. High efficiency of benzoporphyrin derivative in the photodynamic therapy of pigmented malignant melanoma. *Br. J. Cancer* 79(5-6), 821–824 (1999).

46.  Davids LM, Kleemann B, Cooper S, Kidson SH. Melanomas display increased cytoprotection to hypericin-mediated cytotoxicity through the induction of autophagy. *Cell Biol. Int.* 33(10), 1065–1072 (2009).

47.  Sharma SK, Dai T, Kharkwal GB *et al.* Drug discovery of antimicrobial photosensitizers using animal models. *Curr. Pharm. Des.* 17(13), 1303–1319 (2011).

48.  Bouchet A, Serduc R, Laissue JA, Djonov V. Effects of microbeam radiation therapy on normal and tumoral blood vessels. *Phys. Med.* 31(6), 634–641 (2015).

49. Park HJ, Griffin RJ, Hui S, Levitt SH, Song CW. Radiation-induced vascular damage in tumors: implications of vascular damage in ablative hypofractionated radiotherapy (SBRT and SRS). *Radiat. Res.* 177(3), 311–327 (2012).

50. Star WM, Marijnissen HP, Van Den Berg-Blok AE, Versteeg JA, Franken KA, Reinhold HS. Destruction of rat mammary tumor and normal tissue microcirculation by hematoporphyrin derivative photoradiation observed *in vivo* in sandwich observation chambers. *Cancer Res.* 46(5), 2532–2540 (1986).

51. Castano AP, Demidova TN, Hamblin MR. Mechanisms in photodynamic therapy: part three-photosensitizer pharmacokinetics, biodistribution, tumor localization and modes of tumor destruction. *Photodiagnosis Photodyn. Ther.* 2(2), 91–106 (2005).

52. Fingar VH, Siegel KA, Wieman TJ, Doak KW. The effects of thromboxane inhibitors on the microvascular and tumor response to photodynamic therapy. *Photochem. Photobiol.* 58(3), 393–399 (1993).

53. Gilissen MJ, Van De Merbel-De Wit LE, Star WM, Koster JF, Sluiter W. Effect of photodynamic therapy on the endothelium-dependent relaxation of isolated rat aortas. *Cancer Res.* 53(11), 2548–2552 (1993).

54. Henderson BW, Fingar VH. Relationship of tumor hypoxia and response to photodynamic treatment in an experimental mouse tumor. *Cancer Res.* 47(12), 3110–3114 (1987).

55. Kurohane K, Tominaga A, Sato K, North JR, Namba Y, Oku N. Photodynamic therapy targeted to tumor-induced angiogenic vessels. *Cancer Lett.* 167(1), 49–56 (2001).

56. Chen B, Pogue BW, Goodwin IA *et al.* Blood flow dynamics after photodynamic therapy with verteporfin in the RIF-1 tumor. *Radiat. Res.* 160(4), 452–459 (2003).

57. Cramers P, Ruevekamp M, Oppelaar H, Dalesio O, Baas P, Stewart FA. Foscan uptake and tissue distribution in relation to photodynamic efficacy. *Br. J. Cancer* 88(2), 283–290 (2003).

58. Chen B, Roskams T, De Witte PA. Antivascular tumor eradication by hypericin-mediated photodynamic therapy. *Photochem. Photobiol.* 76(5), 509–513 (2002).

59. Zhen Z, Tang W, Chuang YJ *et al.* Tumor vasculature targeted photodynamic therapy for enhanced delivery of nanoparticles. *ACS Nano* 8(6), 6004–6013 (2014).

60. Perentes JY, Wang Y, Wang X *et al.* Low-dose vascular photodynamic therapy decreases tumor interstitial fluid pressure, which promotes liposomal doxorubicin distribution in a murine sarcoma metastasis model. *Transl. Oncol.* 7(3), 393–399 (2014).

61. Inoue K, Fukuhara H, Kurabayashi A *et al.* Photodynamic therapy involves an antiangiogenic mechanism and is enhanced by ferrochelatase inhibitor in urothelial carcinoma. *Cancer Sci.* 104(6), 765–772 (2013).